Scientific
Research

Fracture Toughness Studies of Polypropylene - Clay Nanocomposites and Glass Fibre Reinfoerced Polypropylene Composites

A. Ramsaroop, K. Kanny, T. P. Mohan

Composites Research Group, Department of Mechanical Engineering, Durban University of Technology, Durban, South Africa.
Email: kannyk@dut.ac.za

ABSTRACT

In this paper, a comparative study on the fracture toughness of woven glass fibre reinforced polypropylene, chopped glass fibre reinforced polypropylene and nanoclay filled polypropylene composites is presented. Nanoclays (Cloisite 15A) of 1 wt. % to 5 wt. % were filled in polypropylene (PP) matrix and they were subjected to fracture toughness studies. The specimen with 5 wt. % nanoclay showed 1.75 times and 3 times improvement in critical stress intensity factor (KIC) and strain energy release rate (GIC), respectively, over virgin PP. On the other hand, 3 wt. % nanoclay PP composites showed superior crack containment properties. These structural changes of composite specimens were examined using Transmission Electron Microscopy (TEM) and X-ray diffraction (XRD) methods. It showed that exfoliated nanocomposite structures were formed up to 3 wt. % nanoclay, whereas, intercalated nanocomposite structures formed above 3 wt. % nanoclay in the PP matrix. Furthermore, the woven fibre reinforced PP composites demonstrated superior crack resistant properties than that of clay filled nanocomposites and chopped fibre PP composites. However, KIC and GIC values for woven fibre composites were lesser than that of chopped fibre composites. Moreover, KIC and GIC values for both nanoclay filled PP composites and woven fibre composites are comparable even though the clay filled PP demonstrated catastrophic failure. Also, the crack propagation rate of PP-nanoclay composites is comparable to that of chopped fibre composites.

Keywords: *Fibre Reinforced Composites, Polymer Clay Nanocomposites, Stress Intensity Factor, Crack Growth, Crack Initiation, Fracture Toughness*

1. Introduction

Fibre reinforced plastics (FRP) are commonly used in aerospace, automotive and other engineering applications mainly because of their high strength-to-weight ratio, high stiffness, good resistance to fatigue, and corrosion resistance. Reinforced fibres are usually added in the form of continuous or chopped fibres in a polymer matrix. Each type of these reinforcement fibres has their benefits and limitations in applications. A short fibre reinforced composites can have better processing properties and can be mouldable into complex shaped components. Long fibre reinforced composites, on the other hand, provide enhanced strength and stiffness properties as per the desired directions. Various types of synthetic and natural fibres reinforced plastics are presently studied in literature, namely, glass fibre, carbon fibre, boron, alumina, oxide/carbide and sisal/jute based fibres in a polymer matrix [1-5].

In addition to these fibre reinforced composites, particle reinforced polymer composites are also widely investigated. In these particle filled composites, various types of nano- and micro-scale particles are used. Nanoparticle reinforced polymer composites gained special attention due to their superior and improved properties when compared to their corresponding micro-scale particles. Nanoclays, carbon nanotubes and alumina/oxide based particles are widely used as nanoparticle reinforcements in polymer matrices [6-8]. Polymer-Clay Nanocomposites (PCN) is a relatively new area of research in particle filled composites, and consists of nanoclay as the reinforcement and a polymer serves as the matrix material.

Smectic clays, particularly montmorillonite (MMT) minerals, serve as good nanoclay fillers owing to their ease of dispersion in the organic matrix. MMT consists of nanosized layers of alumina/silicate sheets where the

alumina sheets are sandwiched between two silicate sheets thus causing a net negative charge. This charge is counterbalanced by exchangeable metal ions present in the surface of the layers. MMT clays are generally hydrophilic in nature and can be converted into organophilic by replacing the exchangeable metal ions with cations such as alkylamonium cations. The addition of small amounts of clay (~3 to 5 wt.%) in an organic polymer matrix leads to improved mechanical, thermal and barrier properties.

The addition of nanoclays in a polymer matrix may result in the formation of two types of nanocomposite structures, namely, intercalated and exfoliated nanostructures. In an intercalated structure, the host polymer matrix enters into the interlayer spacing of the nanoclay and increases the interlayer spacing but maintains the parallel arrangement of the nanolayers of clay in the matrix. If the nanolayers of clays are randomly dispersed in the matrix, then the structure is called an exfoliated structure. In practice, exfoliated structures provide enhanced and improved properties due to their excellent dispersions and improved aspect ratio. If MMT clay is not subjected to any surface treatments, then when it is added into a polymer matrix, no nanolayer dispersions of the clay takes place and it acts as a micro-scale filler particle with meagre improvements in properties [9-12].

Polypropylene-clay based nanocomposites are of tremendous research interest due to the improved properties with low clay content as well as the clay serving as a valuable cost effective additive. In general, 0 to 5 wt.% of organically treated clay is added in PP polymer matrix. The addition of the nanoclay in the PP matrix increases the thermal stability in air medium, increases physical properties (dimensional stability), improves flame retardant properties (increased thermal-oxidative stability and reduced Heat Release Rate), improves mechanical properties, fracture properties and gas barrier properties. Several studies were conducted with various types of organo clays, clay concentrations and compatabilizers [13-18].

Research into fracture toughness of thermoplastic nanocomposites is not well known and relatively very few studies are available. Siddiqui et al. [19] reported an increase of 26% in flexural modulus and 60% increase in fracture toughness with the addition of 3 wt.% nanoclays. Cotterell et al. [20] have carried out fracture and fracture toughness studies on spherical and platelet like nano structure filled semi-crystalline polymers. They observed that fracture toughness is a complex study in platelet structure which depends on the aspect ratio of clay platelets, orientation and distribution as well as processing effect. Lingyu Sun et al. [21] have completed a review on energy absorption mechanisms of various nanoparticle filled polymer composite systems. The influence of

some key control parameters such as shape and size of nano-fillers, mechanical properties of nano-fillers and matrix materials, interfacial adhesion, interphase characteristics, as well as the volume fraction and dispersion of fillers in the matrix were studied. They observed that for a weak bonding, the nano-filler will dissipate more energy by pull-out or debonding. For strong bonding, the nano-filler will dissipate energy by tension up to fracture of the filler. Weiping Liu et al. [22] have carried out fracture toughness studies in epoxy-clay based nanocomposites. Fracture toughness of this epoxy system has been greatly enhanced with the addition of nanoclays. With the addition of only 4.5 phr of clay, the strain energy release rate of the epoxy was increased 5.8 times from the original value. Martin N. Bureau et al. [23] have studied fracture analysis for PP based polymer at 2 wt.% nanoclay content with various types of coupling agents. They reported that the toughness improvements were attributed to higher voiding stresses and improved matrix resistance attributed to finer, more oriented clay nanoparticles in the matrix polymer. S.C. Tjong and S.P. Bao [24] showed a two-fold increase of impact fracture toughness of the HDPE/2%Org-MMT and HDPE/4%Org-MMT nanocomposites by adding 10%SEBS-g-MA. Yuan Xu and Suong Van Hoa [25] observed an 85% increase in interlaminar fracture toughness of Carbon Fibre Reinforced Epoxy Nanoclay composites with the introduction of 4 phr nanoclay in epoxy.

Crack initiation and propagation in composites occurs as a result of the three basic fracture modes; which include the opening mode (Mode I), the sliding shear mode (Mode II), and the scissoring shear mode (Mode III). In order to predict crack initiation and propagation, a material's fracture toughness needs to be determined. This is usually expressed in terms of the critical stress intensity factor, KIC, KIIC and KIIIC. In this study, Mode I type testing was carried out for PP-nanoclay composite series. From the literature it was found that structural changes taking place in polymer clay nanocomposites due to varying nanoclay content and their resultant characteristic features of fracture toughness and the analysis of their merits and demerits are relatively scarce. Moreover this new PCN material class will be encountered in various structural loading in practical applications, and hence studying their fracture toughness properties is essential. The objective of this paper is to study the Mode I fracture type of nanoclay filled PP composites with various concentrations (0 to 5 wt.%). The effect of nanoclay on Mode I type fracture toughness is studied and the characteristics of failure is examined by studying the structural changes taking place in the nanocomposites by TEM and XRD techniques. Furthermore, the fracture toughness behaviour of these nanocomposites is com-

pared with woven glass fibre and chopped glass fibre reinforced PP composites. Their merits and demerits of KIC characteristics are discussed in this work.

2. Experimental Studies

2.1. Materials

Cloisite 15A clay was obtained from Southern Clay Products Inc, USA. This is natural montmorillonite clay that was organically treated with a quaternary ammonium salt. The organic modifiers used were dimethyl, dihydrogenatedtallow, quaternary ammonium salt. Polypropylene pellets (melting point 168°C) were procured from Chempro, South Africa. Woven rovings of S2 glass fibre and chopped S2 glass fibre (length 15 mm and diameter of 1 m) were purchased from Vetrotex, S.A.

2.2. Composite Preparation

The nanocomposite panel was manufactured using a melt blending technique. In this technique, the polypropylene pellets and the nanoclay of desired weight concentration (1, 2, 3, 4 and 5 wt. %) were combined in a REIFFEN-HAEUSER screw extruder. The extruder has a 40 mm diameter single rotating screw with a length / diameter ratio (L/D) of 24 and driven by a 7.5 kW motor. Three heating zones along the length of the screw were set up to gradually heat the pellet/clay mixture. The temperatures in these zones were as follows: Zone 1 (pellet loading end) was set at 170°C, Zone 2 (centre region of screw) was at 190°C, and Zone 3 (extrusion end) was maintained at 210°C. This temperature gradient setup was created to avoid thermal shock.

For the preparation of PP-glass fibre (chopped and woven) composites panel, the fibre weight fraction for both these composite structures was 0.3. In the woven fibre polypropylene composites, 4 layers of woven S2 glass fibre were used as the reinforcement. The panels were manufactured using a compression moulding technique. The mould temperature was set at 170ºC and mould pressure was maintained at 20 kN. The chopped fibre composites were also produced using the compression moulding technique at 170°C and 20 kN mould pressure.

2.3. Characterization

The structure of the nanocomposites was studied by using XRD and TEM studies. A Philips PW1050 diffractometer was used to obtain the X–Ray diffraction patterns using CuKα lines (λ = 1.5406 Å). The diffractograms were scanned from 2.5˚ to 12˚ (2θ) in steps of 0.02˚ using a scanning rate of 0.5˚/min. X-ray diffrac-

trograms were taken on Cloisite 15A clay particles and on polypropylene clay nanocomposites. Microscopic investigation of selected nanocomposite specimens at the various weight compositions were conducted using a Philips CM120 BioTWIN transmission electron microscope with an operation voltage of 20 to 120 kV. The specimens were microtomed using a LKB/Wallac Type 8801 Ultramicrotome with Ultratome III 8802A Control Unit. Ultra thin transverse sections, approximately 80-100 nm in thickness were sliced at room temperature using a diamond coated blade. The sections were supported by a 100 copper mesh grid sputter-coated with a 3 nm thick carbon layer.

2.4. Testing

Single edge notch beam (SENB) tests were performed using Lloyds tensile testing machine fitted with a 20kN load cell and at a cross-head speed of 1 mm/min. The ASTM D 5045 testing standard was used for fracture toughness studies. The dimension of the test specimen for plane strain conditions is shown in **Figure 1**. The length (S) of the test specimen is 150 mm with an initial crack length of 5 mm. Five specimens of each composite type were tested and the average values were reported. Also, the standard deviation of test values within 3% is only considered for average value measurements. Mode I stress intensity factor, KI, of the composite specimens was determined as per equation (1), where f(a/W) is a correction factor in accordance standard. The fracture surface was examined using JEOL JSM 840A scanning electron microscope (SEM).

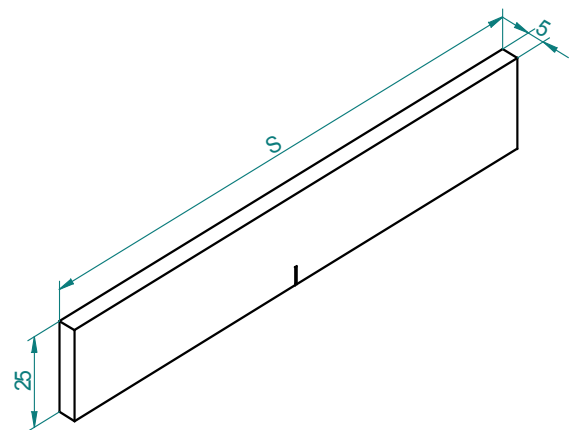$$K_I = \frac{P}{B\sqrt{W}} f\left(\frac{a}{W}\right) \tag{1}$$

Figure 1. Dimensions of SENB specimen that satisfy plane strain conditions.

3. Results and Discussions

3.1. Structure and Morphology of PP-Clay Nanocomposites

The structure and morphology of nanoclay filled PP composites was examined using XRD and TEM methods. **Figure 2** shows the XRD patterns of PP-clay series. The Cloisite 15A nanoclay shows a diffraction peak of 2θ at 3.3° and corresponds to an interlayer spacing of nanoclay (d-spacing) of 26.75Å (calculated from Bragg's diffraction law of 2dSinθ = nλ). From 1 wt.% to 3 wt.% of nanoclay in the PP polymer, there is an absence of a diffraction peak, and this suggests that the matrix polymer has entered into the interlayer spacing of the nanoclay and increased the original nanoclay spacing above the level of 7.5 nm (in which Bragg's law cannot satisfy), or the nanolayers of clays could have randomly dispersed in the PP polymer. Hence, it can be concluded that the nanoclays in the PP polymer from 1 to 3 wt.% formed an ordered exfoliated structure, or a randomly dispersed clay exfoliated structure. Above 3 wt.% nanoclay onwards, there exists a diffraction peak in the composite specimens. In PP with 4 wt.% nanoclay, the nanoclay diffraction peak shifted to a lower 2θ value of 2.68° and this corresponds to an interlayer of clay of 33.5Å. At 5 wt.% nanoclay, the diffraction peak occurs at a 2θ value of 2.9° and corresponds to the interlayer spacing of nanoclays of 30.5Å. XRD results for 4 wt.% and 5 wt.% nanoclay shows that the composite formed intercalated nanocomposite structures.

To further study the dispersion of nanoclays in the PP polymer, TEM morphology of the samples was examined. **Figure 3** shows the bright field TEM images of PP-nano-
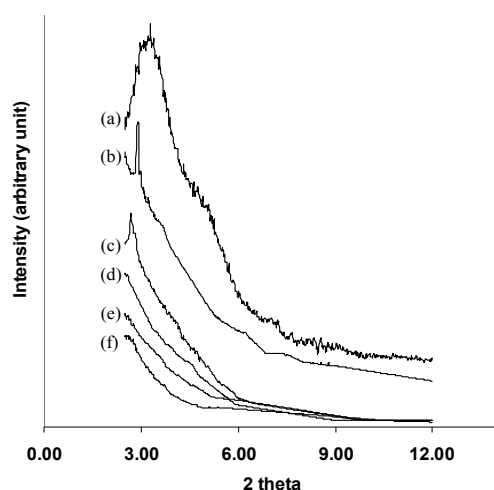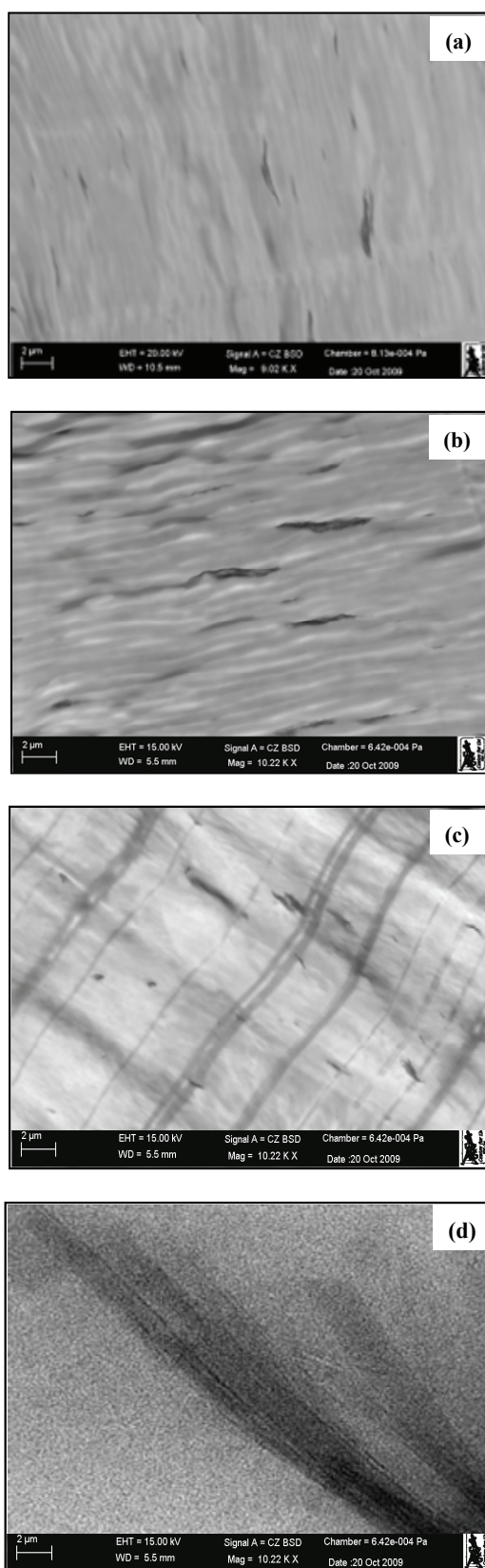
Figure 2. XRD patterns of (a) Cloisite 15A, PP with (b) 5 wt.% clay, (c) 4 wt.% clay, (d) 3 wt.% clay, (e) 2 wt.% clay and (f) 1 wt.% clay.
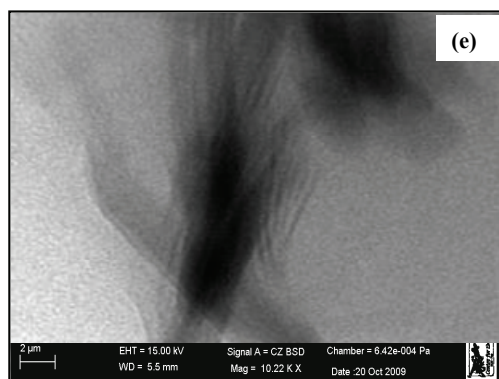
Figure 3. TEM pictures of PP with (a) 1 wt.%, (b) 2 wt.%, (c) 3 wt.%, (d) 4 wt.% and (e) 5 wt.% nanoclay.

Table 1. Average Failure Load, Critical Stress Intensity Factor and Strain Energy Release Rate values for clay weight loadings of 0, 1, 2, 3, 4 and 5%.

Material	Failure Load (N)	Critical Stress Intensity Factor K_{IC} (MPa $\sqrt{m}$)	Strain energy release rate G_{IC} (kJ/m^2)
PP	275	2.00	16.0
PP + 1 wt.% clay	373	2.75	24.3
PP + 2 wt.% clay	480	3.17	29.7
PP + 3 wt.% clay	560	4.09	36.3
PP + 4 wt.% clay	708	4.56	42.1
PP + 5 wt.% clay	768	5.49	48.3

clay composite series. The bright region of the picture is the matrix phase and the dark region is the particle phase. From 1 wt.% to 3 wt. % nanoclay in the PP polymer matrix, the nanolayers of clays were well separated and dispersed randomly in the polymer matrix. This shows the formation of an exfoliated structure. In 4 wt.% and 5 wt. % nanoclay in the PP matrix, the nanolayers of clays were arranged parallel to each other in the PP matrix and this shows the formation of intercalated nanocomposite structures. The TEM pictures support the XRD results for the nanocomposite series.

3.2. Fracture Toughness

3.2.1. Fracture Toughness of Nanocomposite Structures

SENB tests were performed on virgin and nano-reinforced polypropylene structures infused with 1, 2, 3, 4 and 5 wt.% of Cloisite 15A. All tests were conducted under Mode I test conditions and the critical stress intensity factor (KIC), strain energy release rate (GIC) and other related properties for each nanoclay infused structure was determined and is shown in **Table 1**. The table shows that the addition of nanoclays in the PP polymer continuously increased the failure load, KIC and GIC values with increasing clay content. Maximum improvement of KIC and GIC of 1.75 times and 2.66 times, respectively, was observed in the 5 wt.% nanoclay filled PP composite when compared with the virgin PP polymer. Even though the addition of nanoclay continuously increased the KIC and GIC values, the rate of increase was slower at higher clay concentrations (3 wt.% and above). This slower rate increase was possibly due to the formation of intercalated aggregates of nanoclay particles in the PP matrix. The exfoliated structures contributed more toughness properties towards the loading directions due to the increase of the net aspect ratio; whereas in the intercalated

structure, the net and effective aspect ratio was reduced and hence contributed less fracture toughness properties towards the loading direction.

Figure 4 shows the crack propagation versus time of the nanocomposite series. PP shows a propagation of cracks at a relatively shorter time period than nanoclay filled composite specimens. Time for crack propagation increased as nanoclay content increases in the PP polymer up to 3 wt.%, and above 3 wt.% nanoclay content the crack propagation time reduced. Even though KIC of the composite series continuously increased as clay content increased in the matrix, the nanoclay concentrations of above 3 wt.% contributed less towards crack confinement due to their structural features. The crack propagation rate for 3%, 4% and 5% nanoclay composites were 3.53 mm/min, 3.83 mm/min and 3.58 mm/min, respectively. Crack propagation rate for virgin PP was 8.62 mm/min. To understand this behaviour, the fractured surface of these composite specimens was investigated using the SEM process.
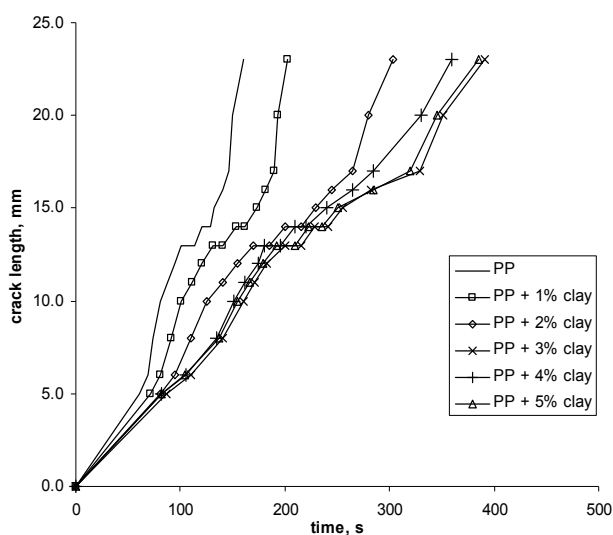

Figure 4. Crack Length versus Time responses for PP and PP-clay composite series.

Figure 5 shows the SEM images of the fractured surface of composite specimens. Pure PP and PP with 5 wt. % nanoclay shows a smooth fracture surface. This failure mechanism is characteristic of a brittle material suggesting that the material had undergone a reduced deformation under failure. However, the SEM image of PP with 3 wt.% nanoclay does not show any brittle type failure mechanism, but rather show extended and elongated deformations before failure. This deformation mechanism possibly induced more time for crack to failure. Furthermore, the exfoliated nanocomposite structure (up to 3
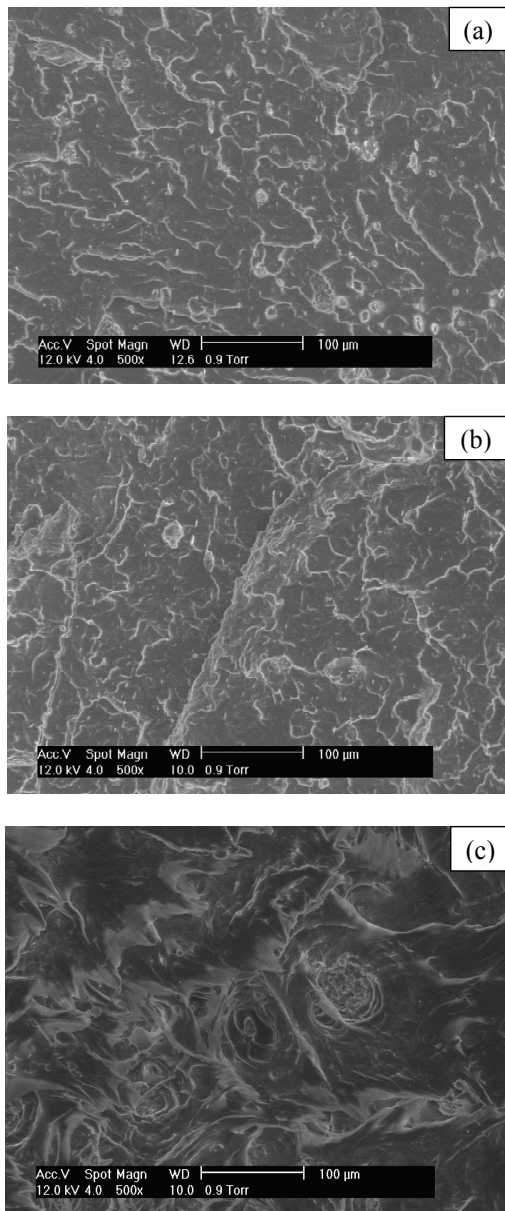
wt. % clay) forced cracks to undertake torturous paths whereas the intercalated structure provided brittle-like failure. This result further suggests that there existed a structural change in the nanocomposite as clay content increased in the PP polymer matrix. Moreover, Ho *et al.* [26] and Moodley *et al*. [27] found that the nanoclay addition improved hardness values, and hence, in our results, the improved hardness values also could have resulted in the improved fracture toughness properties.

3.2.2. Fracture Toughness – Fibre-Reinforced Polypropylene Composites

The two fibre-reinforced composite types (Polypropylene/Chopped S2 Glass and Polypropylene/Woven S2 Glass) were tested under Mode I conditions via the SENB test to establish the crack propagation rates, K_{IC} and G_{IC}. **Figure 6** illustrates the specimen loading with regards to laminate orientation in the woven fibre composites. The loading was perpendicular to the plane of the fibre layers.

The load versus stress intensity factor (K_I) of the composite series is shown in **Figure 7**. It shows that the chopped fibre specimen exhibited a superior load versus K_{IC} response than the other composite materials. The chopped fibre coupon achieved a critical stress intensity factor (K_{IC}) (initiation) of 7.92 MPa√m at a load of 960 N, while a K_{IC} (initiation) value of 5.78 MPa√m at a load of 700 N was obtained in the woven fibre case. Also, the strain energy release rate is superior for chopped fibre reinforced PP composites as shown in **Table 2**.

The poor failure loading performance of the woven fibre composite was due to a "kinking" phenomenon as shown in **Figure 8**. The "kinking" observed on the top-edge of the test coupon in **Figure 8(a)** occurred directly beneath the loading point and directly above the crack front, as shown in **Figure 8(b)**. This occurrence was unnoticeable in the chopped fibre specimens and also in the nanoclay filled PP composites. This caused significant
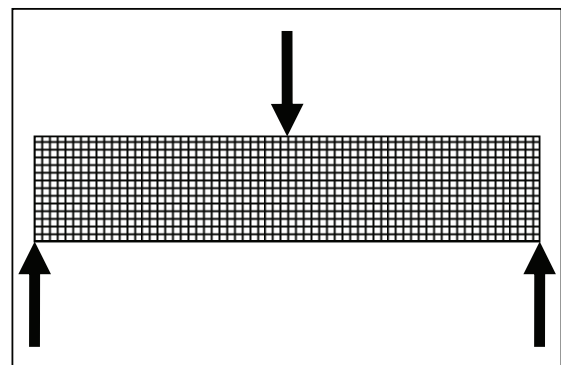
Figure 5. SEM of fractured surface of (a) PP, (b) PP with 5 wt.% nanoclay and (c) PP with 3 wt. % nanoclay.

Figure 6. Illustration showing specimen loading with regards to laminate orientation.

Table 2. Fracture toughness properties of fibre reinforced composites.

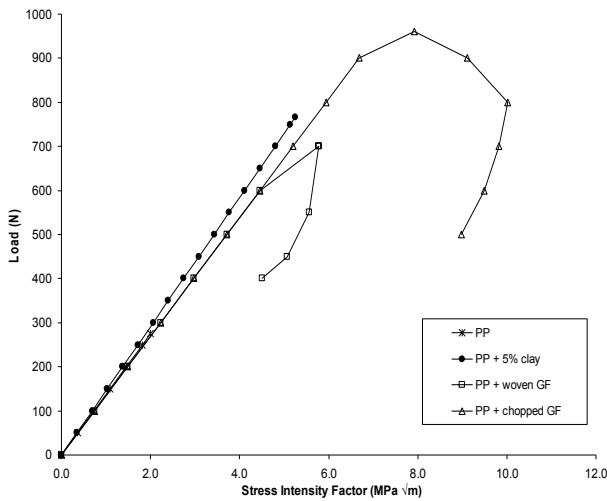| Material	Failure Load (N)	Critical Stress Intensity Factor K_{IC} (MPa $\sqrt{m}$)	Strain energy release rate G_{IC} (kJ/m^2)
PP + chopped GF	960	7.92	181
PP + woven GF	700	5.78	51

Figure 7. Load versus Stress Intensity Factor responses for Polypropylene / Chopped S2 Glass and Polypropylene / Woven S2 Glass.
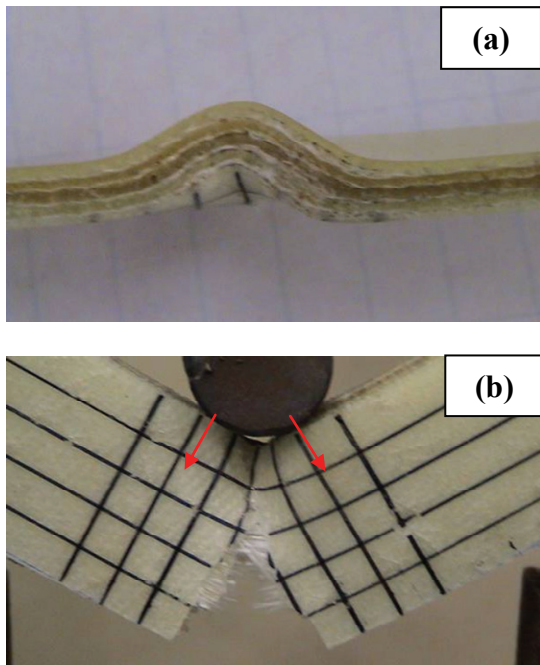

Figure 8. Photographs of Polypropylene/Woven S2 Glass specimen after SENB test showing "kinking" phenomenon from (a) top edge and (b) front surface.

local stresses to be induced at the loading point. Although these stresses were not greater than the breaking stress of the fibres, it was greater than the matrix threshold. Thus the matrix succumbed to the induced localised stresses and was compressed by the test fixture, with no evidence of fibre damage. Upon further loading the stress concentration at the crack front increased to the point where it was large enough to initiate crack growth. Due to the test fixture compression of the coupon, the applied load was not directly above the crack front anymore but applied to adjacent areas as depicted by the arrows in **Figure 8(b)**.

A comparison of crack propagation rates was conducted to determine which composite type had superior crack containment properties. **Figure 9** shows the relationship between Crack Length versus Time for the chopped and woven fibre-reinforced, and the nanoclay filled polypropylene specimens. For all specimens, the crack initiated directly beneath the loading point, which is typical of a Mode I crack. The chopped fibre composites and nanoclay filled composites experienced rapid crack growth compared to the slow crack growth of the woven fibre case. The crack propagation rate for the chopped fibre and 5wt.% nanoclay filled samples were 3.37 mm/min and 3.58 mm/min, respectively, while the woven fibre case had a crack propagation rate of 1.08 mm/min. The woven fibre specimen therefore demonstrated superior crack containment properties as it had a lower crack propagation rate. This containment may be attributed to the structured fibre layout of the Polypropylene/Woven S2 Glass composite. Even though kinking occurred in woven fibre composites, they demonstrated superior crack arresting properties. Moreover, another
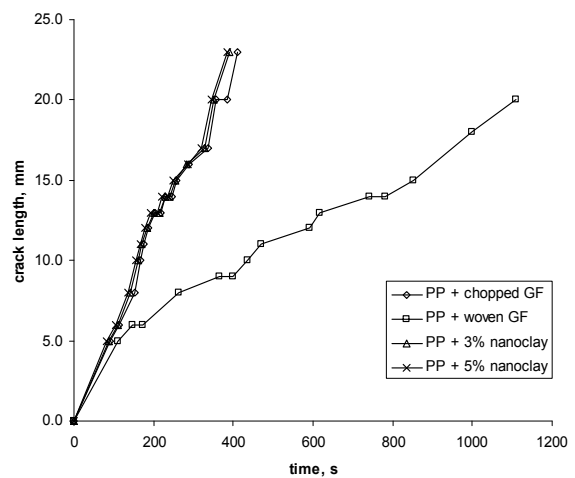

Figure 9. Crack length versus Time responses for PP/ Chopped fibre, PP/Woven fibre and nanoclay (3% and 5 wt.%) filled PP composites.

MSA

interesting observation was that the crack propagation rate was comparable in the nanoclay filled composites and the chopped fibre composites.

Although the nano-reinforced polypropylene showed poor crack containment, the 5 wt.% specimen was able to bear a higher load than the woven fibre specimen. This nanocomposite had a critical stress intensity factor of 5.49 MPa√m, and was 5% less than the woven fibre case which had a critical stress intensity factor of 5.78 MPa√m. This suggests that the 5 wt.% nanocomposite has a similar ability to resist crack initiation as a woven fibre structure with 6 times the reinforcement weight. This characteristic should be considered more important, because a material with a high resistance to crack initiation can sustain higher loads. Such a material may be used in applications where high tensile/flexural loading conditions are prominent.

4. Conclusions

PP polymer filled with nanoclay at various concentrations (1, 2, 3, 4 and 5 wt.%) was prepared by using melt blending extrusion method. It was observed that up to 3 wt.% nanoclay in the PP matrix, an exfoliated structure was formed and further addition of nanoclay formed an intercalated structure. Even though the KIC and GIC values continuously increased as clay content increased in the nanocomposites, the rate of increase was reduced at higher clay content due to intercalated structures that affected the net aspect ratio of the clay platelets.

In the second stage, KIC and GIC were measured for chopped fibre and woven fibre reinforced PP composites. The results showed that the chopped fibres demonstrated an enhanced load bearing capacity and higher fracture toughness values. However, in terms of crack arresting, the woven fibre reinforced PP composites showed superior improvement over the chopped fibre composites. On comparing all three types of composites, the nanocomposite with 5 wt.% clay loading was able to bear a higher load than the woven fibre case, and also demonstrated a comparable critical stress intensity factor with that of the woven glass fibre-reinforced composites. Moreover, the crack arresting properties can be comparable for nanocomposites (3 wt.% and 5 wt.% nanoclay PP composites) and the chopped fibre composites. One of the important points that were noticed was that the weight of fibre reinforcement was 6 times more than the nanoclay weight in the nanocomposite.

REFERENCES

[1] J. Karger-Kocsis, T. Harmia and T. Czigany, "Com-

parison of the Fracture and Failure Behavior of Polypropylene Composites Reinforced by Long Glass Fibers and by Glass Mats," *Composites Science and Technology*, Vol. 54, No. 3, 1995, pp. 287-298.

[2] J. Liakus, B. Wang, R. Cipra and T. Siegmund, "Processing–Microstructure-Property Predictions for Short Fiber Reinforced Composite Structures Based on a Spray Deposition Process," *Composite Structures*, Vol. 61, No. 4, 2003, pp. 363-374.

[3] S. W. Jung, S. Y. Kim, H. W. Nam and K. S. Han, "Measurements of Fiber Orientation and Elastic-Modulus Analysis in Short-Fiber-Reinforced Composites," *Composites Science and Technology*, Vol. 61, No. 1, 2001, pp. 107-116.

[4] H.-Y. Cheung, M.-P. Ho, K.-T. Lau, F. Cardona and D. Hui, "Natural Fibre-Reinforced Composites for Bioengineering and Environmental Engineering Applications," *Composites Part B*: *Engineering*, Vol. 40, No. 7, 2009, pp. 655-663.

[5] G. Ben-Dor, A. Dubinsky and T. Elperin, "An Engineering Approach to Shape Optimization of Impactors against Fiber-Reinforced Plastic Laminates," *Composites Part B*: *Engineering*, Vol. 40, No. 3, 2009, pp. 181-188.

[6] M. Bhattacharya and A. K. Bhowmick, "Polymer–Filler Interaction in Nanocomposites: New Interface Area Function to Investigate Swelling Behavior and Young's Modulus," *Polymer*, Vol. 49, No. 22, 2008, pp. 4808-4818.

[7] T. A. Rajesh and D. Kumar, "Recent Progress in the Development of Nano-Structured Conducting Polymers/ Nanocomposites for Sensor Applications," *Sensors and Actuators B*: *Chemical*, Vol. 136, No. 1, 2009, pp. 275-286.

[8] L. Kumari, T. Zhang, G. H. Du, W. Z. Li, Q. W. Wang, A. Datye and K. H. Wu, "Thermal Properties of CNT-Alumina Nanocomposites," *Composites Science and Technology*, Vol. 68, No. 9, 2008, pp. 2178-2183.

[9] D. Sikdar, D. R. Katti, K. S. Katti and R. Bhowmik, "Insight into Molecular Interactions between Constituents in Polymer Clay Nanocomposites," *Polymer*, Vol. 47, No. 14, 2006, pp. 5196-5205.

[10] B. Xu, Q. Zheng, Y. H. Song and Y. G. Shangguan, "Calculating Barrier Properties of Polymer/Clay Nanocomposites: Effects of Clay Layers," *Polymer*, Vol. 47, No. 8, 2006, pp. 2904-2910.

[11] P. Meneghetti and S. Qutubuddin, "Synthesis, Thermal Properties and Applications of Polymer-Clay Nanocomposites," *Thermochimica Acta*, Vol. 442, No. 1-2, 2006, pp. 74-77.

[12] G. Scocchi, P. Posocco, A. Danani, S. Pricl and M. Fermeglia, "To the Nanoscale, and Beyond: Multiscale Molecular Modeling of Polymer-Clay Nanocomposites," *Fluid Phase Equilibria*, Vol. 261, No. 1-2, 2007, pp. 366-374.

[13] J. G. Zhang, D. D. Jiang and C. A. Wilkie, "Polyethyl-

ene and Polypropylene Nanocomposites Based upon an Oligomerically Modified Clay," *Thermochimica Acta*, Vol. 430, No. 1-2, 2005, pp. 107-113.

[14] Q. Yuan, S. Awate and R. D. K. Misra, "Nonisothermal Crystallization Behavior of Polypropylene–Clay Nanocomposites," *European Polymer Journal*, Vol. 42, No. 9, 2006, pp. 1994-2003.

[15] D. Garcia-Lopez, O. Picazo, J. C. Merino and J. M. Pastor, "Polypropylene–Clay Nanocomposites: Effect of Compatibilizing Agents on Clay Dispersion," *European Polymer Journal*, Vol. 39, No. 5, 2003, pp. 945-950.

[16] Y. Dong and D. Bhattacharyya, "Mapping the Real Micro/Nanostructures for the Prediction of Elastic Moduli of Polypropylene/Clay Nanocomposites," *Polymer*, Vol. 51, No. 3, 2010, pp. 816-824.

[17] L. Raka, G. Bogoeva-Gaceva, K. B. Lu and J. Loos, "Characterization of Latex-Based Isotactic Polypropylene/Clay Nanocomposites," *Polymer*, Vol. 50, No. 15, 2009, pp. 3739-3746.

[18] L. Cauvin, D. Kondo, M. Brieu and N. Bhatnagar, "Mechanical Properties of Polypropylene Layered Silicate Nanocomposites: Characterization and Micro-Macro Modelling," *Polymer Testing*, Vol. 29, No. 2, 2010, pp. 245-250.

[19] N. A. Siddiqui, R. S. C. Woo, J.-K. Kim, C. C. K. Leung and A. Munir, "Mode I Interlaminar Fracture Behavior and Mechanical Properties of CFRPs with Nanoclay-Filled Epoxy Matrix," *Composites Part A*: *Applied Science and Manufacturing*, Vol. 38, No. 2, 2007, pp. 449-460.

[20] B. Cotterell, J. Y. H. Chia and K. Hbaieb, "Fracture Mechanisms and Fracture Toughness in Semicrystalline Polymer Nanocomposites," *Engineering Fracture Mechanics*, Vol. 74, No. 7, 2007, pp. 1054-1078.

[21] L. Y. Sun, R. F. Gibson, F. Gordaninejad and J. Suhr, "Energy Absorption Capability of Nanocomposites: A Review," *Composites Science and Technology*, Vol. 69, No. 14, 2009, pp. 2392-2409.

[22] W. P. Lui, S. V. Hoa and M. Pugh, "Fracture Toughness and Water Uptake of High-Performance Epoxy/Nanoclay Nanocomposites," *Composites Science and Technology*, Vol. 65, No. 15-16, 2005, pp. 2364-2373.

[23] M. N. Bureau, M.-T. T.-T. and F. Perrin-Sarazin, "Essential Work of Fracture and Failure Mechanisms of Polypropylene-Clay Nanocomposites," *Engineering Fracture Mechanics*, Vol. 73, No, 16, 2006, pp. 2360-2374.

[24] S. C. Tjong and S. P. Bao, "Fracture Toughness of High Density Polyethylene/SEBS-g-MA/Montomorrilonite Nanocomposites," *Composites Science and Technology*, Vol. 67, No. 2, 2007, pp. 314-323.

[25] Y. Xu and S. Van Hoa, "Mechanical Properties of Carbon Fibre Reinforced Epoxy/Clay Nanocomposites," *Composites Science and Technology*, Vol. 68, No. 3-4, 2008, pp. 854-861.

[26] V. K. Moodley and K. Kanny, "Characterization of Polypropylene Nanocomposite Structures," *Journal of Engineering Materials and Technology*, Vol. 40, 2007, pp. 1-8.

[27] K. Lau, M. Ho, C. Lam, H. L. Ng and D. Hui, "Mechanical Properties of Epoxy-Based Composites Using Nanoclays," *Composites Structures*, Vol. 75, No. 1-4, 2006, pp. 415-421.